Available online at www.sciencedirect.com

ScienceDirect

Physics Procedia 3 (2010) 343–350

Physics Procedia

www.elsevier.com/locate/procedia

International Congress on Ultrasonics, Universidad de Santiago de Chile, January 2009

Phonon attenuation in the GHz regime: Measurements and simulations with a visco-elastic material model

Juerg Bryner*, Timothy Kehoe[a,b], Jacqueline Vollmann, Laurent Aebi, Ingo Wenke, Jurg Dual

Institute of Mechanical Systems, Department of Mechanical and Process Engineering, ETH Zurich,CH-8092 Zurich, Switzerland
[a] Catalan Institute of Nanotechnology and (ICN-CIN2), Campus Bellaterra - Edifici CM7, 08193-Bellaterra (Barcelona), Spain
[b] Tyndall National Institute, University College Cork, Cork, Ireland

Abstract

Aluminum and PMMA thin film samples are investigated regarding their mechanical properties like speed of sound and attenuation. Aluminum is often used as a transducer layer for pump probe laser measurements and different PMMA types have a large importance in the nanoimprinting technique. The measurements are performed on a short pulse laser pump probe setup, where bulk wave packets in the GHz regime are excited and detected using near infrared laser pulses of less than 100 fs duration. This contact-free and non-destructive measurement method is explained. In order to extract the attenuation precisely from the measurements, the entire experimental setup is simulated numerically: The heat distribution and the thermo-elastic wave excitation caused by the laser pulse, the mechanical wave propagation, and the photo-acoustic detection. By means of the visco-elastic modeling of the wave propagation, the simulations are fitted to the measurements by tuning the attenuation parameters in the numerical model. In this way it is possible to extract the attenuation from the measurements. First, two different types of Aluminum on a sapphire substrate are analyzed: Electron beam evaporated Aluminum and sputtered Aluminum, respectively. The thicknesses of the Aluminum films are in the range of 300 nm. It turns out that the attenuation is much higher in the sputtered Aluminum film. Afterwards, PMMA thin films used for nanoimprinting with thicknesses between 300 and 600 nm are analyzed. The PMMA thin films are spincoated onto a Silicon wafer and covered with an Aluminum transducer layer. The very good agreement between the measurements and simulations of the stacked samples allows a reliable determination of the attenuation in the PMMA films in the GHz regime.

Keywords: Bulk acoustic waves; laser acoustics; phonon attenuation; thin film metrology; wave propagation

1. Introduction

Recently, in nanoimprinting research there is a growing need for the mechanical characterization of polymer films and structures. The laser acoustic method as introduced by Thomsen et al. [1], [2] is well known and widely

* Corresponding author. Tel.: +41-44-6325293; fax: +41-44-6321145.
E-mail address: juerg.bryner@imes.mavt.ethz.ch.

doi:10.1016/j.phpro.2010.01.045

used in the semiconductor industry, mostly for measurements on metallic specimens, e.g. interconnects of computer chips. Thomsen et al. also presented a complete modeling of the laser acoustic measurement procedure that can be divided into three parts: The calculation of the temperature distribution in the specimen, the linear elastic calculation of the wave propagation, and the calculation of the photoacoustic detection. With this modeling Thomsen et al. had a good agreement with experimental data for Arsenic Telluride and Nickel films. Later Morath et al. [3] investigated phonon attenuation in PMMA and other polymer films in the GHz regime. By comparing the ratios of certain peaks in the experimental data and in the linear elastic simulation they were able to determine the attenuation. In this paper a new approach for the determination of the attenuation is used. The wave propagation in all layers is simulated using a visco-elastic material model. By fitting the numerical results to the experimental data the attenuation in the layers is determined.

2. Experiment

2.1. Pump probe laser setup

For the measurements presented here, a pump probe setup is used. A description of pulse laser pump probe measurements is given by Vollmann et al. [4]. A pulse laser generates very short light pulses (<100 fs) with a repetition rate of 81 MHz and a wavelength of 800 nm. By a beam splitter, the laser beam is separated into a pump and a probe beam, which are used for the excitation and detection of acoustic pulses in the structure to be inspected, see Fig. 1. A variable delay line with a retroreflector in the pump beam path enables a very precise control of the temporal shift between the pump and the probe pulses arriving at the surface of the specimen. Moving the delay line 1 µm corresponds to a time shift of 6.7 fs between the pump and the probe pulse. In order to reduce optical cross-talk, the polarization of the probe beam is turned around 90 degrees by a λ/2 plate. By a polarizing beam splitter the pump and probe beam are realigned and guided in a collinear manner through a microscope objective and focused to the surface of the specimen. The diameter of the focused beam at the surface is estimated to be in the order of 10 µm. A camera is used for the adjustment of the two beams.

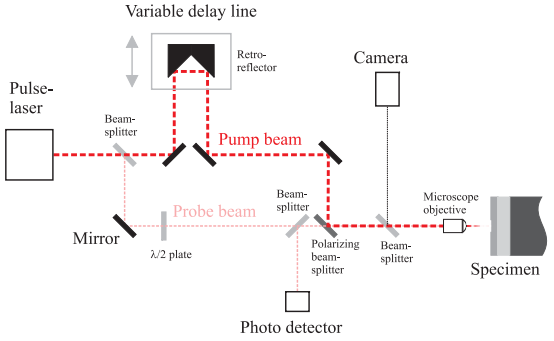

Fig.1 Main components of the pump probe laser setup.

The pump pulse causes a fast temperature increase near the surface. This generates mechanical stress that starts to propagate mainly as a one-dimensional bulk wave into the specimen. At every interface of the layered specimen the waves are partly reflected thus heading back to the surface. Near the surface, the mechanical waves cause a small

change of the optical reflectivity at the surface. This is called the photoacoustic effect. Superimposed to the photoacoustic effect, there is also a change in the optical reflectivity caused by the temperature rise at the surface. The optical reflectivity is recorded with a photo-detector that measures the intensity of the reflected probe beam.

With this measurement the time of flight of the bulk wave pulses through the thin film layers is determined. If the material properties determining the bulk wave velocity are known, with the time of flight the thickness of the corresponding layer can be calculated. Or vice versa, for a known thickness, the bulk wave velocity can be calculated. Furthermore, by the analysis of the height and the shape of the peaks in the optical reflectivity data, the phonon attenuation can be determined.

2.2. Direct analysis of the measurement data

Typical data of a single layer measurement are shown in Fig. 2. The acoustic contribution to the reflectivity change is plotted in the upper diagram. The first and the second echo are named $\Delta R_1(t)$ and $\Delta R_2(t)$, respectively. The magnitudes of the Fourier transforms of the two echoes $\Delta R_1(t)$ and $\Delta R_2(t)$ are plotted in the lower diagram.

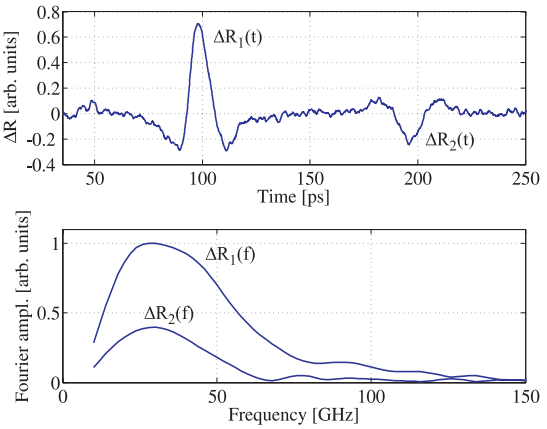

Fig.2 Upper diagram: Acoustic contribution to the reflectivity change versus time for a 304 nm Al film deposited by E-beam evaporation on a sapphire substrate; lower diagram: Fourier transforms of the two echoes in the upper diagram

Thomsen et al. [1] introduced the following formula for the determination of the attenuation α directly from the data in Fig. 2:

$$\alpha(f) = \frac{1}{2d} ln\left(\frac{r_{FS} \Delta R_1(f)}{\Delta R_2(f)} \right) \qquad (1)$$

α is the attenuation, f the frequency, d the film thickness, and r_{FS} the bulk force reflection coefficient. The application of formula (1) is simple but requires two successive echoes and there must be no overlap between these

echoes. These conditions are satisfied for the measurements of the single Al layers with thicknesses in the range of 300 nm as presented in Fig. 2. The results of these measurements are discussed in section 4.

3. Modeling and simulation

The laser acoustic experiment is modeled with a one-dimensional simulation model covering three main parts (Fig. 3) which are described in detail in the following sections.

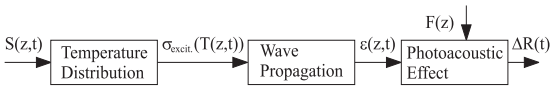

Fig.3 Simulation model: laser power density S, stress σ, strain ε, reflectivity change ΔR, and sensitivity function F.

3.1. Temperature distribution

In the first part of the simulation the temperature distribution in the top metal layer heated by the laser pulse is calculated with the two temperature model described by Qiu et al. [5]. The two temperature model takes into account that the electron temperature and the lattice temperature are not in an equilibrium due to the fast heating process. This leads to a nonlinear system of two equations:

$$C_e(T_e)\frac{\partial T_e}{\partial t} = \frac{\partial}{\partial z}\left(K_e(T_e)\frac{\partial T_e}{\partial z}\right) - G(T_e - T_l) + S(z,t) \tag{2}$$

$$C_l\frac{\partial T_l}{\partial t} = G(T_e - T_l) \tag{3}$$

C_e is the heat capacity of the electrons, T_e is the temperature of the electrons, t is the time, z is the spatial coordinate, K_e is the thermal conductivity, G is the electron-phonon coupling factor, T_l is the temperature of the lattice, S is the laser power density, and C_l is the heat capacity of the lattice. For both the electrons and the lattice adiabatic boundary conditions are applied, thus neglecting the heat transfer into the air and the polymer layer:

$$\left.\frac{\partial T_e}{\partial z}\right|_{z=0} = \left.\frac{\partial T_e}{\partial z}\right|_{z=L} = \left.\frac{\partial T_l}{\partial z}\right|_{z=0} = \left.\frac{\partial T_l}{\partial z}\right|_{z=L} = 0 \tag{4}$$

L is the thickness of the top metal layer. The equations are solved numerically using a finite difference code. The spatial discretisation is done with second order central differences. The explicit Euler scheme is used for the temporal integration.

The temperature distribution determines the excitation stress $\sigma_{excit.}$, that launches a mechanical wave:

$$\sigma_{excit.} = -\alpha(3\lambda + 2\mu)(T_l - T_0) \tag{5}$$

α is the thermal expansion coefficient, λ and μ are the Lamé constants, and T_0 is the reference temperature.

3.2. Wave propagation

The wave propagation is calculated in the second part of the simulation. In this paper a viscoelastic material model is used (Christensen [6]): The standard linear solid. It is represented by two Hookean springs, E_1 and E_2 and a Newtonian damper η. Its representation is shown in Fig. 4. σ is the stress, and ε is the strain.

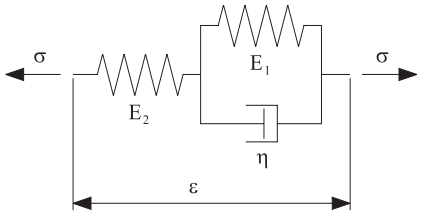

Fig.4 Standard linear solid.

The dynamic behavior of a visco-elastic solid is completely defined by its creep compliance function, which looks as follows for the standard linear solid:

$$J_c(t) = \frac{E_1 + E_2}{E_1 E_2} - \frac{1}{E_1} e^{-\frac{E_1}{\eta} t} \tag{6}$$

Three useful substitutions are introduced: E_0, E_∞, and T_0.

$$E_0 = E_2 \tag{7}$$

$$E_\infty = \frac{E_1 E_2}{E_1 + E_2} \tag{8}$$

$$T_0 = \frac{\eta}{E_1} \tag{9}$$

E_∞ can be interpreted as the effective modulus for low frequencies ($f \ll 1/T_0$), E_0 can be interpreted as the effective modulus for high frequencies ($f \gg 1/T_0$), and T_0 is the time constant of the exponential creep compliance function. The frequency dependent attenuation α in the standard linear solid can be calculated analytically from the three parameters E_0, E_∞, and T_0. This is shown in (10) to (13). The complex Young's Modulus E^* of a standard linear solid is defined by (10):

$$E^*(f) = E_\infty + \frac{(E_0 - E_\infty) i 2\pi f}{\frac{E_0}{E_\infty T_0} + i 2\pi f} \tag{10}$$

E^* can be decomposed in a real part E', the storage modulus, and in an imaginary part E'', the loss modulus:

$$E^*(f) = E'(f) + iE''(f) \tag{11}$$

The quality factor Q then is defined by the ratio of E' and E''. Q corresponds to the number of wavelengths, after which a mechanical pulse has reduced its magnitude by a factor of e^{π} :

$$Q(f) = \frac{E'(f)}{E''(f)} = \frac{E_0 + E_\infty T_0^2 (2\pi f)^2}{(E_0 - E_\infty) T_0 2\pi f} \tag{12}$$

The attenuation α is directly related to the quality factor by (13):

$$\alpha(f) = \sqrt{\frac{\rho}{E'(f)}} \frac{\pi f}{Q(f)} \tag{13}$$

The one-dimensional wave propagation in a standard linear solid is described by a set of three equations:

$$\frac{\partial \sigma}{\partial z} = \rho \frac{\partial^2 u}{\partial t^2} \tag{14}$$

$$\varepsilon = \frac{\partial u}{\partial z} \tag{15}$$

$$\varepsilon(t) = J_c(0)\sigma(t) + \int_0^t \dot{J}_c(t)\sigma(t-\tau)d\tau \tag{16}$$

ρ is the density and u is the displacement. Equation (14) is Newton's equation, (15) is the kinematic relation, and (16) is the constitutive law for visco-elastic materials. At the surface of the specimen the stress free boundary condition is applied:

$$\sigma_{z=0} = 0 \tag{17}$$

Equations (14) - (16) are solved with the piecewise-linear recursive-convolution method as described by Taflove and Hagness [7]. This method uses finite differences on a staggered grid in space and time.

3.3. Photoacoustic effect

In the third part of the simulation the photoacoustic effect, i.e. the optical reflectivity change at the surface $\Delta R(t)$ is calculated. The reflectivity change at the surface depends on the so called sensitivity function $F(z)$ (see Thomsen et. al. [1]) and the strain distribution $\varepsilon(z,t)$:

$$\Delta R(t) = \int_0^\infty F(z)\varepsilon(z,t)dz \tag{18}$$

4. Results

4.1. Aluminum films

Al films are important for pump probe measurements because they are often used as a transducer layer on the top of the layer of interest. The attenuation in the Al layer influences the amplitude and shape of all wave packets, also of those which are used for the analysis of the attenuation in the underlying layers of interest. Two different types of Al are compared regarding their attenuation: A 304 nm thick Al film deposited by E-beam evaporation (Fig. 2) and a 319 nm thick sputtered Al film. Both Al films are deposited on a sapphire wafer. The bulk wave velocities of the two Al types are calculated with the measured thickness at a reference point (profilometry measurements) and the measured time-of-flight at the same point (measurements with the pump probe laser setup). The bulk wave velocity

of the E-beam deposited Al film is determined to be 6200 m/s and the velocity of the sputtered Al film is determined to be 5873 m/s. The other parameters used for the analysis are taken from the literature: The density of Al 2700 kg/m^3, the density of sapphire 3980 kg/m^3, and the bulk wave velocity of sapphire 11476 m/s. The attenuation α then is determined directly from the measured reflectivity according to formula (1) at 30 GHz, which is the main frequency of the mechanical pulses (see Fig. 2). α is found to be 2600 cm^{-1} for the E-beam deposited Al and 8900 cm^{-1} for the sputtered Al film. A series of measurements confirms that the attenuation α in the sputtered Al film is about a factor of 3 higher than in the Al film deposited by E-beam evaporation for frequencies in the range of 30 GHz. These results show that in Al thin films there is a significant attenuation that also influences the wave packets traveling through the underlying layers.

4.2. PMMA films

The specimens considered in this section consist of a PMMA layer spincoated onto a Silicon wafer. On the PMMA layer there is sputtered an aluminum top layer (about 60 nm thick) which is used as transducer for the excitation and detection with the laser. The direct analysis of the measurement data according to formula (1) is not possible for these kinds of specimens because the echoes overlap each other. Here the simulation procedure described in section 3 incorporating a visco-elastic material model is used in order to determine the attenuation α .

By a combination of profilometry and pulse laser measurements the bulk wave velocities in the Al and PMMA layers are determined to be 5737 m/s and 2644 m/s, respectively. The other parameters used for the analysis are taken from literature: The density of Al 2700 kg/m^3, the density of PMMA 1012 kg/m^3 (datasheet from the supplier), the bulk wave velocity of Silicon (100) 8447 m/s, and the density of Silicon 2329 kg/m^3. Using these parameters two specimens are investigated regarding their attenuation α : A 346 nm thick PMMA layer (see Fig. 5) and a 590 nm thick PMMA layer. Both measurements are optimally fitted by using the same attenuations in the simulations. For the about 60 nm thick sputtered Al top layers the attenuation α is found to be 20500 cm^{-1} at 50 GHz, which is the main frequency of the mechanical pulses in these specimens. Assuming a quadratic relation between attenuation and frequency this is a plausible value compared to 8900 cm^{-1} for the sputtered Al at 30 GHz in the previous section. For the PMMA layers of both specimens (346 nm and 590 nm) α is found to be 22600 cm^{-1} at 50 GHz. Again, assuming a quadratic relation between attenuation and frequency, this result is in good agreement with the measurements done by Morath et al. [3] for frequencies between 90 and 320 GHz.

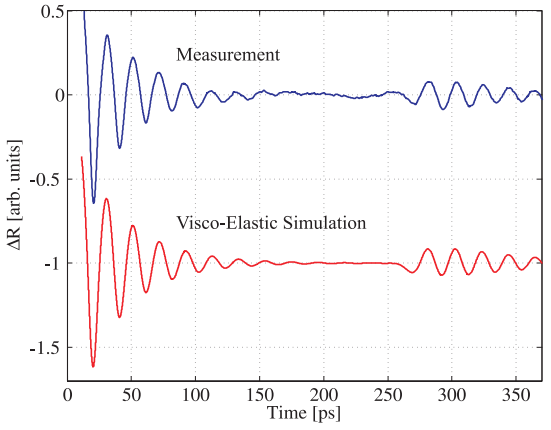

Fig.5 Acoustic contribution to the reflectivity change of a 59 nm Al - 346 nm PMMA - Si specimen: Measurement and visco-elastic simulation with attenuation α_{Al} = 20500 cm^{-1} and α_{PMMA} = 22600 cm^{-1} at 50 GHz.

5. Conclusions

The analysis of the attenuation in two different Al thin films shows that there is a significant attenuation that must not be neglected in simulations for the determination of the attenuation in underlying thin films. It also turns out that the attenuation in the sputtered Al film is about a factor of 3 higher than in the Al film deposited by E-beam evaporation for frequencies in the range of 30 GHz. For the determination of the attenuation in PMMA layers a new approach is used. The entire laser acoustic measurement is simulated numerically using the visco-elastic standard linear solid for the wave propagation. The simulations are fitted to the measurements by tuning the attenuation α . For two different specimens having PMMA layers with thicknesses of 346 nm and 590 nm the same value of the attenuation leads to a very good matching between simulations and measurements. In the PMMA layers the attenuation α is found to be 22600 cm^{-1} at 50 GHz.

Acknowledgment: This work is partly supported by the EC-funded project NaPANIL (Contract No. NMP2-LA-2008-214249)

References

[1] C. Thomsen, H. T. Grahn, H. J. Maris, J. Tauc "Surface generation and detection of phonons by picosecond light-pulses" Physical Review B, vol. 34, pp. 4129-4138, 1986.
[2] C. Thomsen, H. J. Maris, J. Tauc "Picosecond acoustics as a non-destructive tool for the characterization of very thin films" Thin Solid Films, vol. 154(1-2), pp. 217-223, 1987.
[3] C. J. Morath, H. J. Maris "Phonon attenuation in amorphous solids studied by picosecond ultrasonics" Physical Review B, vol. 54(1), pp. 203-213, 1996.
[4] J. Vollmann, D. M. Profunser, J. Dual "Sensitivity improvement of a pump-probe set-up for thin film and microstructure metrology" Ultrasonics, vol. 40(1-8), pp. 757-763, 2002.
[5] T. Q. Qiu, C. L. Tien "Short-pulse laser-heating on metals" International Journal of Heat and Mass Transfer, vol. 35(3), pp. 719-726, 1992.
[6] R. M. Christensen "Theory of Viscoelasticity" Academic Press, 1971.
[7] A. Taflove, S. C. Hagness "Computational electrodynamics, the finite-difference time-domain method" Artech House, Boston London, 2005.